A New Look at RF Power Requirements in MRI

T. S. Ibrahim[1], L. Tang[1], D. Abraham[1]

[1]Electrical and Computer Engineering, University of Oklahoma, Norman, OK, United States

Introduction: As human MRI is performed at higher field strengths, the issue of RF power deposition/frequency dependence [1,2] becomes highly critical. The main difficulty in accurately describing a correlation between power requirements and operating frequency is due to the inhomogeneity of RF fields at high field strengths. As a result, there is extreme ambiguity in obtaining well defined conclusions in regards to this issue. In this work, we closely study the RF power/frequency dependence up to frequencies nearing 12 T on a variety of electrical load sizes, configurations, and RF coils. More importantly, we provide power relations associated with the use of RF shimming to achieve ***highly homogenous RF fields with a fixed uniformity criteria*** at B_0 field strengths up to 9.4 T for human head imaging.

Methods: A 3D human head model loaded within a 16-strut TEM resonator was utilized in full 3D FDTD calculations ranging from 4T to 9.4T (details of the model are shown in Fig. 1). In addition, to study a case that validates the typical quasi-static approximations, we considered a single strut TEM element with an electrically small load (9.4 cm long cylinder phantom with a 4.6 cm diameter and filled with material having the following properties: dielectric constant = 78 and conductivity = 1.154 S/m). This case was also modeled using the FDTD method. All of the power and B_1^+ field calculations were done on the 5 axial slices (A1-A5) shown in Fig. 1, under various B_0 magnetic field strengths (4T, 5T, 7T, 8T, and 9.4T). The optimizations of the B_1^+ field were done in the aforementioned 5 slices using 4-, 8-, and 16-port excitations.

Results and Discussion: Fig. 2 describes the power requirements for the case of the single strut and electrically small load. As expected, the results show that the power is proportional to the square of the operating frequency up to approx. 12T. The results are also identical for the excite (B_1^+) field as well as the receive field (which has opposite circular polarization to that of the B_1^+ field). This verifies the predicted quasistatic approximation for the specified electrically small (dimensions << the operating wavelength) load.

When examining the results in the human head, however, the power dependence is considerably different. Fig. 3 shows the power dependence of the fixed phase/amplitude (P/A) excitation using 8- and 16-ports. It is clearly shown that the square dependence of the power on frequency vanishes to become 1) linear in the slices towards the bottom of the brain (A1-A3), or 2) peak-then-decrease in slices towards the top of the brain. The results also show that the use of more drive ports with this excitation scheme results in a slight reduction of the power requirements.

When utilizing optimized P/A excitation, the nature of the power dependence is different from that of the fixed P/A. First, as shown in Fig. 3, optimization for B_1^+ field homogeneity results in increased power requirements. On the other hand, the peak-then-decrease relation observed with the upper brain slices with the fixed P/A excitation becomes more evident in the lower brain slices as well. Fig. 4 describes the power dependence to achieve homogeneity equal to the most homogenous B_1^+ field in slice A3 at 9.4 T using 4 ports, at all other field strengths and using 8- and 16-port excitation. The results clearly show that to achieve a specified criteria of homogeneity for the B_1^+ field distribution, the use of more drive ports (and therefore more phase-locked transmit channels) will significantly reduce the RF power required to achieve a specified B_1^+ field intensity. Several other numerical studies were conducted and verified these findings.

References: [1] Collins, C. M. and Smith, M. B., *MRM*, 45, 684-91, 2001. [2] Ibrahim, T. S., *IEEE Trans. Microwave. Th. Tech.*, 1999-03, 2004.

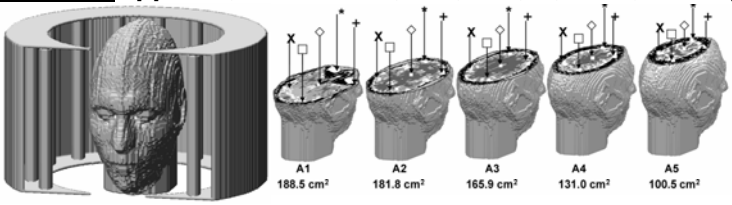

Fig. 1: Anatomically detailed head model loaded within the TEM resonator. The 5 head cuts show the orientation of 5 slices (A1-A5) used in power and B_1^+ field calculations (Figs. 3, 4). On each slice, 5 points were picked where the B_1^+ field was calculated with the FDTD method.

Fig. 2: Power required to obtain a specified average flip angle over the volume of a 9.4 cm long and 4.6 cm in diameter cylindrical phantom filled with tissue-like dielectric properties.

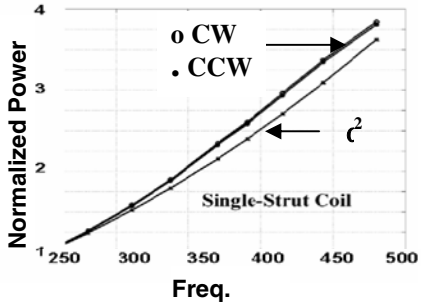

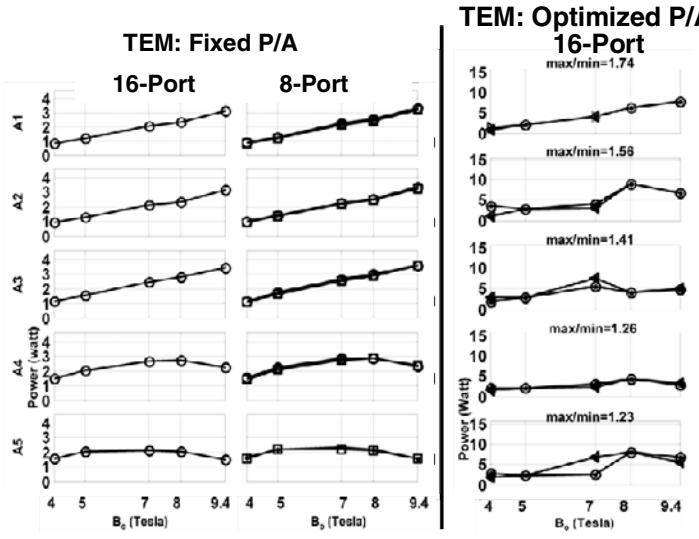

Fig. 3: Plots of power absorbed in the head required to achieve a fixed mean B_1^+ field value (1.174 micro tesla over the area of each of the 5 slices shown in Fig. 1) as a function of B_0 field. In the optimized cases, each ***max/min*** denotes the same "Maximum B_1^+ field intensity over Minimum B_1^+ field intensity" at all field strengths within a particular slice.

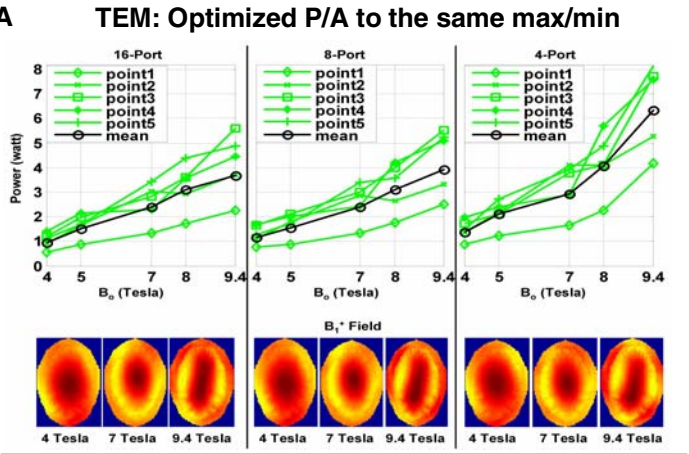

Fig. 4: Top: Absorbed power comparison under different 16-, 8-, and 4-ports driving conditions. The results are presented for slice A3 (Fig. 1). The values on each sub-plot correspond to the power required to achieve a mean B_1^+ field value = 1.174 micro tesla (across the slice). The power values at all frequencies and under all the driving conditions were calculated for the same B_1^+ field homogeneity (***max/min*** = 1.70) which represents the best possible solution achieved using a 4-port optimized P/A driving condition. Bottom: B_1^+ field distributions in slice A3 at 4, 7 and 9.4 Tesla for the same field homogeneity.